Int. J. Heat Mass Transfer. Vol. 27, No. 12, pp. 2377–2385, 1984
Printed in Great Britain

0017-9310/84 $3.00 + 0.00

The analysis of heat transfer in fixed beds of particles at low and intermediate Reynolds numbers

S. C. DHINGRA,* D. J. GUNN†‡ and P. V. NARAYANAN§

*Department of Chemical Engineering, Indian Institute of Technology, New Delhi, India; †Department of Chemical Engineering, University College, Singleton Park, Swansea, SA2 8PP, U.K.; §Eastman Kodak Co., Rochester, New York

(*Received* 13 *October* 1983 *and in revised form* 30 *April* 1984)

Abstract—The dynamic response to an input pulse, of fixed beds packed with glass ballotini, has been measured over the range of particle Reynolds numbers from 1–300. The thermal conductivity of the particles, the particle to fluid heat transfer coefficient, and the coefficient of axial thermal dispersion have been found by Laplace transform analysis, Fourier transform analysis and by a numerical method, each applied to a minimum variance search. The three methods of estimation are described and compared. Agreement is found to be good over the entire range of Reynolds numbers although the sensitivity of the experiments to axial dispersion was greatest at low Reynolds numbers, while the sensitivity to fluid heat transfer coefficient and intra-particle conductivity was greatest at high Reynolds numbers.

INTRODUCTION

UNTIL fairly recently it has been assumed that experiments for heat transfer into fixed beds may be interpreted in terms of the interaction between convection and heat transfer between the fluid and the surfaces of the particles. If the particles are metallic it is usually permissible to neglect the effect of intra-particle thermal conductivity on the experimental response, but even for beds of non-metallic particles it is usual to neglect the effects of intra-particle thermal conductivity and of axial thermal dispersion. None of the published work in heat transfer to 1965 [1] has included the effects of thermal dispersion and intra-particle thermal conductivity in the analysis of experiments, but subsequently there has been some consideration of the effect of these two properties on thermal response at both low and high Reynolds numbers [2–4]. To suppose that no heat is transferred by conduction in particles and dispersion in fluid in the axial direction leads to some error at high Reynolds numbers, but at low Reynolds numbers very large errors may arise when dispersion is neglected.

The principal experimental method has been frequency response in which the attenuation and phase change of a steady sinusoidal pulse of heat has been examined for different bed lengths. The generation of an accurate sinusoid, while not essential, greatly simplifies the treatment of the experimental results. Such a form of input signal is difficult to arrange, while the generation of a single sharp heat pulse is easier, although the treatment of the experimental results is more complex.

In this paper we report the response of fixed beds to single pulses of heat and compare the results with experimental frequency response. The range of Reynolds numbers was from 1 to 300. The experimental responses were analysed by three different methods. The first two methods were based upon the analytical properties of the experimental Laplace and Fourier transforms, while the third method was based upon a comparison of the experimental responses and numerical solutions to the partial differential equations describing the effects of convection and dispersion within the bed. A preliminary account of some aspects of the transform analysis of the experimental results has been presented [5].

‡ Author to whom correspondence should be addressed.

EXPERIMENTAL METHODS

Figure 1 shows a line diagram of the experimental arrangement. Air was metered by a bank of rotameters before passing through a flanged section at the base of the bed. The air then passed over a tungsten wire 0.025 mm in diameter that was wound over a rectangular Tufnol frame so that a rectangular space of 30×10 mm was spanned by the wire; the resistance

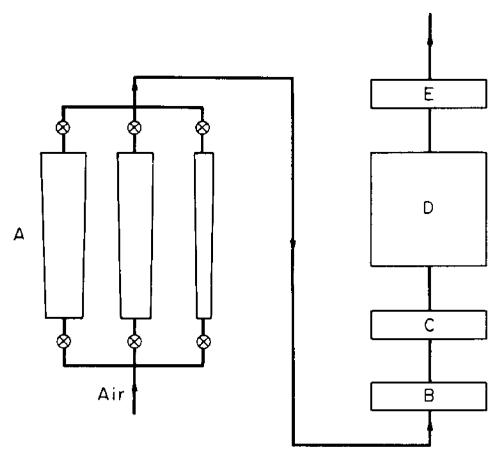

FIG. 1. The experimental arrangement: A, flowmeters; B, E, temperature sensors; C, grid heater; D, test column.

NOMENCLATURE

- c specific heat of fluid at constant pressure [J kg^{-1} K^{-1}]
- c_s specific heat of solid at constant pressure [J kg^{-1} K^{-1}]
- e bed porosity
- $\bar{G}$ Laplace transform of the rate of conduction of heat into a particle for a step change of unity [J]
- h particle to fluid heat transfer coefficient [W m^{-2} K^{-1}]
- K_z axial coefficient of thermal dispersion [W m^{-1} K^{-1}]
- n inward directed normal
- N number of particles per unit volume of solid
- N_A number of axial nodes
- N_R number of particle nodes
- q_c rate of heat conduction into unit volume of solid [W m^{-3}]
- R radial coordinate [m]
- s Laplace transform parameter [s^{-1}]
- t time [s]
- T fluid temperature in bed [K]
- T_p fluid temperature in particle [K]
- T_R reference temperature [K]
- T_S particle surface temperature [K]
- $\bar{T}$ Laplace-transformed temperature [K s]
- $\hat{T}$ Fourier-transformed temperature [K s]
- V interstitial velocity [m s^{-1}]
- w Fourier transform parameter [s^{-1}].

Greek symbols

- α defined by equation (20)
- γ defined by equation (21)
- θ defined by equation (19)
- λ thermal conductivity of solid [W m^{-1} K^{-1}]
- ρ mass density of fluid [kg m^{-3}]
- ρ_s mass density of solid [kg m^{-3}].

of the wire was 9 Ω. Air was directed by means of a wooden conduit over the wire and then through a section of pipe 150 mm long and 88 mm in diameter packed with glass ballotini to a grid heater that spanned the cross-section of the inlet to the packed bed.

The grid heater consisted of 200 strands of 0.025 mm diameter nickel wire, each 50 mm long, attached to two conducting supports, one of which was attached to a taut spring to allow for expansion of the wires on heating. The voltage supplied to the heater was constant but controlled by a timing circuit. In operation 2.8 V was applied across the heater for about 30 s. The period was controlled to give an output pulse that was sharp and of good amplitude. The packed bed was placed directly above the grid heater.

On leaving the bed the gas passed through a slit that was spanned by a tungsten wire 0.025 mm in diameter wound to a resistance of 9 Ω to match the sensor that registered the input temperature of the air. The two sensors were placed in a Wheatstone bridge arrangement that was balanced by a standard resistance wound from manganin wire when no heat was applied to the grid heater. When heat applied from the grid heater reached the upper sensor, the resistance of this tungsten wire was increased, so creating an out-of-balance voltage in the bridge that was fed to a sensitive strip chart recorder that could read to a maximum full scale sensitivity of 50 μV.

The packed bed and immediate ancillaries were insulated because the materials of construction of walls and flanges were Tufnol, Perspex and wood, all materials of low thermal conductivity, so that the radial heat flux was always very small compared to the axial heat flux. The bed was coupled by quick release wrenches to the input heater and the output detector so that the bed in position could be easily replaced.

The change of temperature with time, or the form of a temperature transform in the bed may be determined in theory as the solution to a partial or ordinary differential equation. The parameters of the differential equations were found by comparing the theoretical and experimental temperature distributions or transforms. To determine an accurate temperature distribution from the experiment it was necessary to correct for the end effects of the bed, in particular, effects due to the inlet section, mixing cone and output detector.

The correction was incorporated in the experimental results by using two lengths of bed, each chosen to give a response that could be measured accurately. A bed 30 mm in length containing the particles to be tested was secured between the heater and output sections, and when operating conditions had been stabilized, a voltage was applied to the heater for a predetermined period and the response was recorded. The bed was then replaced by a section of bed 60 mm in length containing similar particles, and when operating conditions were steady, a pulse of heat was applied for exactly the same period. This pulse was also recorded. Thus the original rectangular pulse was arranged to provide two responses, the first of which was the thermal response of the input section, output detector and a bed 30 mm in length, while the second was the response of the end sections and a bed 60 mm in length. As the input pulse to each section was identical it is clear that the response of the larger section differs from the response of the shorter section because of a length of bed equal in length to the difference between the two sections. Thus the first pulse may be regarded as the input, and the second may be regarded as the output response from a bed 30 mm in length, a procedure that corrects for the end sections, although two experiments are required for each result.

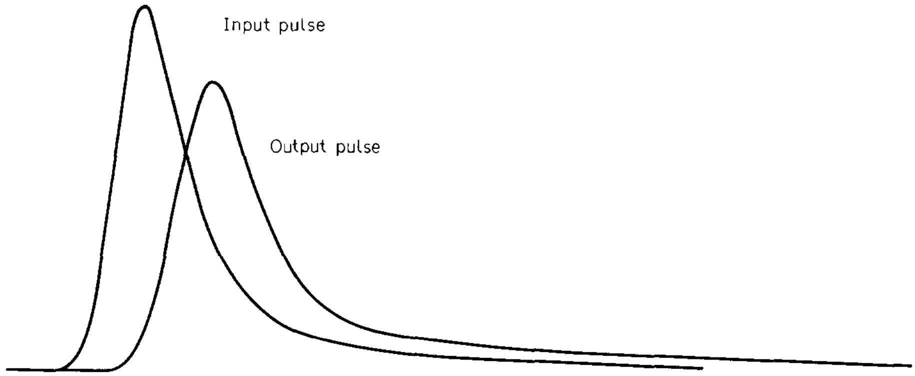

FIG. 2. Typical experimental response.

It was intended to cover a range of Reynolds numbers from 1 to 300 in the experiments, but at low velocities within the bed the attenuation of the pulse was so severe that bed lengths shorter than those employed would have been necessary for an accurate capture of the pulse form. However, by changing the size of particles so that small particles were used for small Reynolds numbers, a good accuracy was maintained. Experiments at the highest Reynolds numbers were carried out with 6 mm diameter lead glass ballotini, at the lowest with 1.15 mm lead glass ballotini and with 3 mm glass ballotini at intermediate Reynolds numbers.

In a typical experiment the desired flow rate of air was set to a fixed bed 30 mm in length and the power supply to the heater was switched on for a period controlled by an electric timer. The output pulse was recorded until the output of the detector bridge had returned to the base level, typically about 1 h. The 30 mm bed was then replaced by a 60 mm bed and the response was again measured. The response to an identical heating pulse is shown in Fig. 2.

The two pulses were digitized at 30 points over the range by means of a Benson–Lehner film analyzer, a device that produced the data for each pulse as a set of punched cards. In this form the pulses could be conveniently analyzed.

THEORY

When the temperature of a fluid passing through a fixed bed is changed, the heat flux at a plane z, $K_z(\partial T/\partial z) - \rho c V T$, if a function of time, will cause a change in the fluid temperature with time $\partial T/\partial t$.

A heat flow into each particle q_c that varies with time, is a consequence of the change in fluid temperature, and the partial differential equation that links the separate quantities is [6]

$$K_z\frac{\partial^2 T}{\partial z^2} - \rho c V\frac{\partial T}{\partial z} - q_c\frac{(1-e)}{e} - \rho c\frac{\partial T}{\partial t} = 0. \quad (1)$$

The rate of conduction q_c is given by the field equations that describe temperature distributions within the particle. Thus if the particles are spherical, the partial differential equation describing a transient field is

$$\lambda\nabla^2 T_p = \rho_s c_s\frac{\partial T_p}{\partial t} \quad (2)$$

with the coupling condition between equations (1) and (2) by continuity conditions at the surface of the particles, so that for spherical particles

$$\frac{\pi d^3}{6}q_c = \pi d^2 h(T - T_p) = \pi d^2\lambda\frac{\partial T_p}{\partial n} \quad (3)$$

where n is the inward directed normal at the particle surface.

An analytical solution to equations (1) and (2) either for a semi-infinite set of conditions

$$T = T_0(t) \quad \text{at} \quad z = 0$$
$$T \to T_a, \quad \text{the ambient temperature at} \quad z \to \infty \quad (4a)$$

or a finite set of conditions

$$Vc\rho T_0 = V\rho c T - K_z\frac{\partial T}{\partial z}, \quad t > 0, \quad T_0 = f(t),$$
$$\frac{\partial T}{\partial z} = 0 \quad \text{at} \quad z = L \quad (4b)$$

has not been found. However, if Laplace and Fourier transforms are taken of equations (1) and (2), a variety of analytical solutions in Laplace and Fourier transform space may be found for several particle shapes [6]. To obtain the shape of the output pulse numerical inversions are required, and because of the difficulties of this step, a ready check of the calculated output and experimental output pulses cannot be made easily.

The response to the finite set of conditions (4b) may be found by numerical methods. Such a solution is demanding because the temperature fields have to be discretized in time t, the axial coordinate z and the particle radial coordinate, and in practice it is sometimes difficult to distinguish between a true feature of the thermal response and an aberration of the numerical method, so that some testing of the consistency of the numerical solution is necessary.

In parameter estimation it is required to vary the parameters of the differential equations until agreement with experimental distributions is found. In applying methods of non-linear regression, analyses in the Laplace-transformed or Fourier-transformed domain have the considerable advantage that analytical solutions to the transformed equations (1) and (2) may be used to compare with experimental transforms, and for this reason the two types of transform analysis were carried out first [5]. However, a more direct comparison of experiment and theory may be obtained by numerical analysis.

NUMERICAL ANALYSIS

Equation (1) is a partial differential equation of mixed parabolic–hyperbolic type for which parabolic behaviour might be expected if K_z is dominant, while hyperbolic behaviour should be found when convection dominates. At high velocities when convection dominates, changes in the temperature field due to convection are more rapid than dispersive changes and with some finite-difference schemes calculation of changes due to dispersion may be masked by finite diffusion errors in the convection terms [7].

Equation (2) is parabolic, and both the backward implicit and the Crank–Nicolson method permit solutions of equation (2) that are without restrictions on stability in one, two or three dimensions. However, in two or three space dimensions the sets of linear equations are no longer tridiagonal in the matrix of coefficients, and therefore the solutions can require a great deal of computational time at finer mesh sizes. If two- or three-dimensional solutions of equation (2) are required, the ADI method in which the finite-difference equations are implicit in one direction only, and explicit in others, with the implicit direction changing each cycle of calculations, will still retain the tridiagonal form of the matrix of coefficients [7]; the solutions are locally second order in both space and time.

At low velocities the dominant form of equation (1) will be parabolic and a backward implicit and a Crank–Nicolson method of solution will give solutions to the coupled equations (1) and (2) that are of unrestricted stability. However, the matrix of coefficients, although banded, requires a dense-matrix algorithm for solution. Although both methods are consistent, the time required for a solution in which further refinement of the space and time increments gave no significant change to the output pulse, and the complete time of solution, including parameter estimation, was very large indeed.

One possibility of reducing computational requirements was to employ the basic idea of ADI methods, but to alternate an implicit and explicit formulation between the bed and the particle temperature fields. The essence of an analysis of stability and convergence is the same as for two-dimensional concentration and temperature fields so that properties of stability and convergence should be similar to the fully implicit method.

In a series of pilot calculations using typical parameter values it was found that satisfactory convergence could be obtained for this method for values of time and space increments that were similar to the fully implicit method. This numerical method could be employed with routines for parameter estimation for computing times that, although still long, were manageable.

Equation (1) in explicit form, when a forward difference is used to represent the time derivative and central differences are used to represent the spatial derivatives, is equivalent to the following expression written for node i

$$T_{i,j+1} = T_{i-1,j}\left(\frac{K_z\Delta t}{\rho c(\Delta z)^2} - \frac{V\Delta t}{2\Delta z}\right) + T_{i,j}\left(1 - \frac{2K_z\Delta t}{\rho c(\Delta z)^2} - \frac{6h\Delta t(1-e)}{\mathrm{d}\rho\, ce}\right) + T_{i+1,j}\left(\frac{K_z\Delta t}{\rho c(\Delta z)^2} + \frac{V\Delta t}{2\Delta z}\right) + \frac{6h\Delta t(1-e)}{\mathrm{d}\rho\, ce} T_{s,j}. \quad (5)$$

The corresponding implicit form is

$$-T_{i-1,j+1}\left(\frac{K_z\Delta t}{\rho c(\Delta z)^2} - \frac{V\Delta t}{2\Delta z}\right) + T_{i,j+1} \times \left(1 + \frac{2K_z\Delta t}{\rho c(\Delta z)^2} + \frac{6h\Delta t(1-e)}{\mathrm{d}\rho\, ce}\right) - T_{i+1,j+1} \times \left(\frac{K_z\Delta t}{\rho c(\Delta z)^2} + \frac{V\Delta t}{2\Delta z}\right) = T_{i,j} + \frac{6h\Delta t(1-e)}{\mathrm{d}\rho\, ce} T_{s,j+1}. \quad (6)$$

Equation (2) is placed in explicit form by expressing the time derivative as a forward difference, and the spatial derivatives as central differences

$$T_{\mathrm{p}i,k,j+1} = T_{\mathrm{p}i,k-1,j}\left(\frac{\lambda\Delta t}{\rho_s c_s(\Delta R)^2} - \frac{\lambda\Delta t}{\rho_s c_s R\Delta R}\right) + T_{\mathrm{p}i,k,j}\left(1 - \frac{2\lambda\Delta t}{\rho_s c_s(\Delta R)^2}\right) + T_{\mathrm{p}i,k+1,j} \times \left(\frac{\lambda\Delta t}{\rho_s c_s(\Delta R)^2} + \frac{\lambda\Delta t}{\rho_s c_s R\Delta R}\right). \quad (7)$$

The corresponding implicit formulation of equation (2) is

$$-T_{\mathrm{p}i,k-1,j+1}\left(\frac{\lambda\Delta t}{\rho_s c_s(\Delta R)^2} - \frac{\lambda\Delta t}{\rho_s c_s R\Delta R}\right) + T_{\mathrm{p}i,k,j+1}\left(1 + \frac{2\lambda\Delta t}{\rho_s c_s(\Delta R)^2}\right) - T_{\mathrm{p}i,k+1,j+1}\left(\frac{\lambda\Delta t}{\rho_s c_s(\Delta R)^2} + \frac{\lambda\Delta t}{\rho_s c_s R\Delta R}\right) = T_{\mathrm{p}i,k,j}. \quad (8)$$

To this set of equations is added the initial condition of ambient (zero) temperature at the start of each experiment together with the boundary conditions

$$V\rho c T_0 = V\rho c T - K_z \frac{\partial T}{\partial z} \quad \text{at} \quad z = 0, t > 0, T_0 = f(t) \quad (9)$$

$$\frac{\partial T}{\partial z} = 0 \quad \text{at} \quad z = L \quad (10)$$

$$\frac{\partial T}{\partial R} = 0 \quad \text{at} \quad R = 0 \quad (11)$$

as well as equation (3).

This set of equations was solved in the order, explicit bed (5), implicit particle (8), explicit particle (7), and implicit bed (6), a sequence that covered two time intervals. The computation was advanced in time using the input pulse $T_0(t)$ until both the input and the output pulse had returned to the ambient temperature condition.

The time interval Δt and the space intervals ΔR and Δz were changed until the outlet pulse was apparently free from significant numerical inaccuracies and a reduction in Δt or Δz for example did not affect the numerical solution. The chosen value of $\Delta z/L$ was 1/21, and of $\Delta R/R_0$ was 1/6.

The explicit equations (5) and (7) were solved by sequential substitution. The sets of implicit equations (6) and (8), when placed in matrix form, have a tridiagonal matrix of coefficients that may be solved by a sequence of forward substitution followed by back substitution, an algorithm that required storage and computational time directly proportional to the number of nodes, and not to the square as in the fully implicit method. The computational time for the entire sequence of calculations is thus proportional to the sum of the intra-particle and extra-particle nodes, a more economic arrangement than the fully implicit analysis where the sparse, banded nature of the matrix of coefficients presented heavier penalties.

Once conditions of numerical integration had been established so that the numerical integration of equations (1) and (2) could be completed without significant numerical error, the parameters K_z, λ and h were found by non-linear regression.

This was done by calculating the output pulse from the numerical solution by selecting temperatures at the same times as employed for digitizing the output pulse from the experimental record. The variance of experimental values about the corresponding theoretical curve was calculated from the expression

$$\sigma^2 = \sum_{i=1}^{m} \left(\left(\frac{T_i}{T_R}\right)_{\text{exp}} - \left(\frac{T_i}{T_R}\right)_{\text{theory}} \right)^2 \Big/ (m-1) \quad (12)$$

where T_R is a convenient reference temperature.

This equation was linked to a computer routine that was programmed to seek the minimum value of σ^2 by changing the values of h, λ and K_z. At the conclusion of a sufficient number of trials, or when the value of σ^2 had been made sufficiently small, the values of the parameters associated with the smallest value of σ^2 were the best values provided by that particular experiment.

TRANSFORM ANALYSIS

If the Laplace transforms of equations (1) and (2) of the boundary conditions are taken, the transform of the output temperature pulse may be expressed [6]

$$\bar{T} = \bar{T}_0 \exp\left[\frac{V\rho c z}{2K_z}\left(1 - \sqrt{\left(1 + \frac{4K_z s}{(V\rho c)^2} \times \left(N\left(\frac{1-e}{e}\right)\bar{G} + \rho c\right)\right)}\right)\right] \quad (13)$$

where $\bar{G}$ is the Laplace transform of the rate of conduction into the particle when the initial condition is one of constant temperature and the surface is raised to unit temperature at $t = 0$. For the spherical particle $\bar{G}$ is given by [6]

$$\bar{G} = \frac{4\pi r^2}{s} \times h\left[\frac{r(s\rho_s c_s/\lambda)\coth(r\sqrt{(s\rho_s c_s/\lambda)}) - 1}{rh/\lambda - 1 + r\sqrt{(s\rho_s c_s/\lambda)}\coth(r\sqrt{(s\rho_s c_s/\lambda)})}\right]. \quad (14)$$

To determine the parameters K_z, h and λ the Laplace transforms $\bar{T}$ and $\bar{T}_0$ were calculated numerically from the experimental responses

$$\bar{T} = \int_0^\infty e^{-st}\, T\, dt. \quad (15)$$

The values of $\bar{T}$ and $\bar{T}_0$ were calculated for several different values of s. The variance of the experimental transforms about the corresponding theoretical values calculated from equations (13) and (14) was then calculated from

$$\sigma^2 = \sum_{i=1}^{m} \left[\left(\frac{\bar{T}}{\bar{T}_0}\right)_{i,\text{expt.}} - \left(\frac{\bar{T}}{\bar{T}_0}\right)_{i,\text{theory}} \right]^2 \Big/ (m-1). \quad (16)$$

This equation was linked to a computer routine in the same manner as that employed for finding the best parameters by numerical analysis of equations (1) and (2) and the experimental responses.

A similar procedure was employed to analyze the dynamic response in the Fourier transform domain. The Fourier transform is defined as

$$\hat{T} = \int_{-\infty}^{\infty} e^{-iwt}\, T(t)\, dt. \quad (17)$$

In terms of the transform the solution is [6]

$$\hat{T} = \hat{T}_0 \exp\left(\left(\left(\frac{V\rho c}{2K_z} - \theta\alpha\right) - i\theta\right)z\right) \quad (18)$$

where

$$\theta = \sqrt{\left(\frac{V^2\rho^2c^2}{8K_z^2} + \frac{p}{2K_z}\right)}\sqrt{(\sqrt{(1+\gamma^2)} - 1)} \quad (19)$$

$$\alpha = \sqrt{\left(\frac{\sqrt{(1+\gamma^2)}+1}{\sqrt{(1+\gamma^2)}-1}\right)} \quad (20)$$

$$\gamma = \frac{4K_z(q + w\rho c)}{V^2\rho^2c^2 + 4pK_z} \tag{21}$$

where p and q represent the real and imaginary parts of the particle response [6].

Equation (16) and the parameter estimation procedure used for both the time and Laplace domain analyses were employed to find the best estimation of the three parameters K_z, h and λ. Several different values of w were chosen and the parameters were varied until the experimental and theoretical dependences agreed.

Thus, from each experiment, three sets of parameters, K_z, h and λ were found by parameter estimation in the time domain, in the Laplace transform domain and in the Fourier domain.

DISCUSSION

Each of the methods of analysis can be relied upon only if the conditions of numerical analysis have been carefully chosen. Thus the space and time increments used in numerical solution of the partial differential equations were changed until reduction of each increment was found not to affect the calculated dynamic response.

The range of values of w in the Fourier transform analysis was chosen to lie below a limit that was found by numerical experiments. For large values of w the effect of experimental error in the pulse response is to give general random fluctuations both in the attenuation ratio and in the phase lag [8]. This effect is so severe in the phase lag that it was found necessary to base the variance [16] upon the attenuation ratio only in the Fourier transform analysis. On the other hand, if the range of w chosen from $w = 0$ was too small parameter interaction was so strong that good estimates of the separate parameters could not be found.

The range of values of s in the Laplace transforms was also found by numerical experimentation upon the experimental responses. For large values of s the transform is so attenuated by the factor e^{-st} that the experimental integrals are sensitive only to the early parts of the experimental response, where the magnitude of the signal is small, while for small values of s the experimental integrals become unduly sensitive to the tails of the experimental responses, where the experimental inaccuracies are large.

Irrespective of the method of analysis the thermal response of the bed at low Reynolds numbers is dominated by axial dispersion, and is relatively insensitive to the heat transfer coefficient and the intraparticle thermal conductivity, while at high Reynolds numbers the response to axial dispersion is much less sensitive. These findings from earlier investigations were confirmed by parameter estimates from each of the three methods.

The typical input and output pulses shown in Fig. 2 contain an extensive region at long times for which the temperature is small with respect to the peak of the pulse. As the experiment was scaled in accuracy to the peak of the pulse, the accuracy of the later stages of the response was not high. In the earlier stages of the experimental work the input detector shown in Fig. 1 was not employed, and it was added at a later stage to improve the steadiness of the base line and to reduce base-line drift. With the input and output detectors in a bridge arrangement there was no significant base-line drift, but because of the rapid attenuation of the pulse even for extremely short bed lengths, it was not possible to produce experimental pulses that were sharply peaked without tailing.

The tailing of the pulse was faithfully reflected in the direct calculations based upon the partial differential equations. Figure 3 is a comparison of a typical experimental output pulse compared with the numerical solution when the parameters had been found by minimum variance search based upon the numerical solutions. The main features of the pulse are reproduced by the numerical analysis, although minor differences are apparent in one or two regions.

All three methods of parameter estimation gave acceptable values of the heat transfer parameters over the entire range of Reynolds numbers once the correct settings had been found for each method, i.e. intervals of integration for the numerical method, range of w for the Fourier transform, and range of s for the Laplace transform. From the initial investigation it was clear that the reliability of each method was acceptable only if the correct settings had been used, and very little reliance could be placed upon parameters found from the numerical solution of the partial differential equation when intervals of axial length and time were too large, or from frequency response when the upper value of w was too high. However, once acceptable

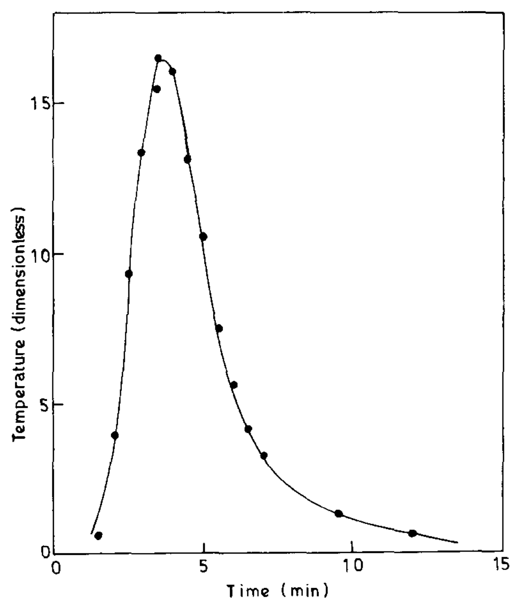

FIG. 3. Comparison of typical experimental output pulse shown as points with pulse calculated by numerical analysis shown as a continuous line.

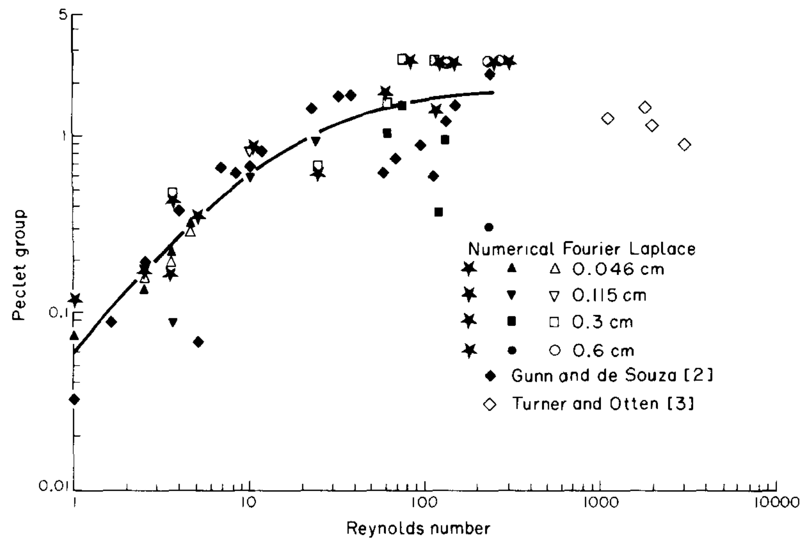

FIG. 4. Dependence of Peclet number upon Reynolds number. The solid line is the estimated average dependence.

settings had been chosen there was a satisfactory agreement between parameters for each of the three methods.

It is known from earlier work that the transport coefficients of a fixed bed may be changed on repacking the bed; thus Pryce [9] obtained a standard deviation of 15% of the mean coefficient of axial dispersion when repacking the bed between measurements, but the standard deviation was only 5% when repeating measurements without repacking. The experimental techniques used in this investigation, particularly because of the need to correct for end effects, effectively required repacking between each set of pulse measurements, so that there is a variability in the experimental results due to repacking.

Figure 4 shows the dependence of the thermal Peclet number upon Reynolds number for the entire set of experimental results; the caption to the figure indicates the size of the glass ballotini used in the experiment, and the method of parameter estimation. At low Reynolds number the coefficient of dispersion tends to a constant value since dispersion is dominated by molecular contributions and the contribution of convection is small. In this region the thermal response is determined by dispersion. At higher Reynolds numbers the contribution of convection to dispersion is greater and the effect of heat transfer coefficient and intra-particle thermal conductivity upon the response is stronger. It is apparent in Fig. 4 that the envelope of estimates of the Peclet group is wider at high Reynolds number, reflecting the fact that the thermal response is less sensitive to axial dispersion at high Reynolds number and therefore the precision of the estimate is less at higher Reynolds number. There is no systematic difference in favour of one method or another at low Reynolds numbers, but at Reynolds numbers in the range of 60–140, both the numerical method, and the Laplace transform method gave estimates at the upper allowed bound of the range; estimates from the Fourier transform did not show this difficulty but a high variability is evident. Included in the data shown on Fig. 4 are the earlier estimates of Gunn and de Souza [2] that extended to low Reynolds number, and of Turner and Otten [3] who measured thermal response at high Reynolds number. The experimental estimates of the three sets of data are evidently consistent.

The estimates of Gunn and de Souza were found from experimental equipment almost identical to that employed in this investigation, but by experimental frequency response instead of the present method of pulse response. The thermal response could be measured to Reynolds numbers as low as 0.06 by experimental frequency response, but it was not possible to estimate parameters from pulse response for Reynolds numbers less than 1. This difference is probably due to the more critical requirements for numerical accuracy of the pulse, where it is necessary to measure the full extent of the pulse; in experimental frequency response it is only necessary to measure the amplitude and phase lag of the peak of the wave. A similar finding has been drawn from comparisons of pulse and experimental frequency response for packed-fluidized beds [10] where experimental frequency response was necessary to extend the study of thermal response to lower Reynolds number.

The estimates of the particle Nusselt group found by the three methods are shown in Fig. 5. The diagram also includes the estimates of Nusselt number due to Gunn and de Souza and Turner and Otten, but only for $Re > 1$ since at low Reynolds number the thermal response is sensitive only to axial dispersion. The lack of sensitivity of the response to the Nusselt group at low Reynolds number is shown by the greater scatter, particularly due to the numerical method. The line on

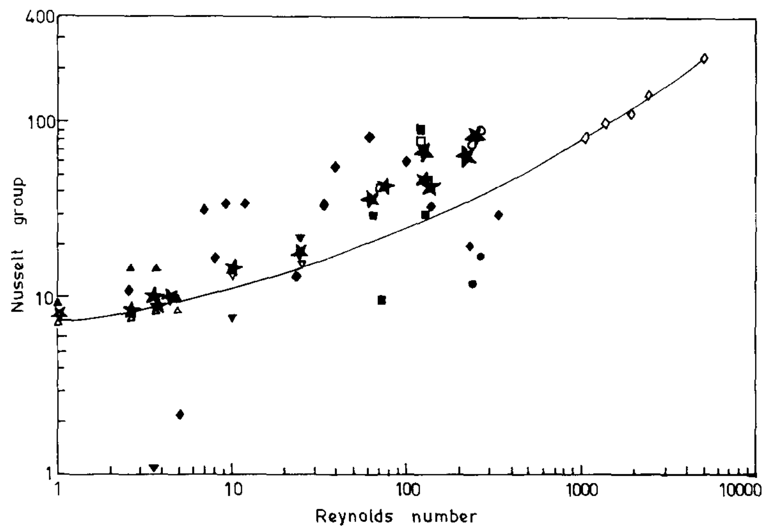

FIG. 5. Dependence of Nusselt number upon Reynolds number. Caption as for Fig. 4. The line corresponds to equation (22).

the figure is an equation for the Nusselt number as a function of porosity, Prandtl and Reynolds number in fixed and other beds of particles [11]

$$Nu = 4(1+0.7Re^{0.2}\ Pr^{1/3})+0.6Re^{0.7}\ Pr^{1/3}. \quad (22)$$

This equation is in satisfactory accord with the data, particularly when it is borne in mind that the scatter is due in part to the methods of estimation.

The neglect of thermal dispersion in the analysis of experiments has a very strong influence at low Reynolds numbers and it is important to bear this in mind when comparing the estimates shown in Fig. 5 with other work. If thermal dispersion is neglected at low Reynolds numbers it may be shown that the Nusselt group will approach zero at a rate proportional to the square of the product of the Reynolds and Prandtl groups [2]; a theoretical equation drawn from this analysis agrees with the estimates of the Nusselt group within the range of Reynolds number from 0.1 to 1.0 drawn from experiments for which it has been assumed that the coefficient of thermal dispersion is zero. As Nusselt groups of the order of 10^{-3} have been reported for experiments in the range of Reynolds number from 0.1 to 1, it is evident that the differences can amount to 2 or 3 orders of magnitude in the Nusselt group.

It may be observed that in addition to the phenomenon of low sensitivity at low Reynolds number, there is sufficient parameter interaction at intermediate Reynolds number that has the effect of introducing a scatter in the reported values of Nusselt and Peclet groups and the intra-particle thermal conductivity; this factor is partly responsible for the variation in experimental results shown in Figs. 4 and 5.

The average values for the thermal conductivity of the glass ballotini were found to be 0.931, standard error 0.101 W m^{-1} K^{-1} by the Laplace transform method, 0.918, standard error 0.105 W m^{-1} K^{-1} by the Fourier transform method, and 0.903, standard error 0.05 W m^{-1} K^{-1} by the numerical method. It was assumed in the parameter estimation that there was an *a priori* expectation of the value of each parameter and therefore according to Bayes theorem [12] the probability of a given result was the product of the likelihood of the observed result and the prior probability. It was assumed that the prior probability density was uniform between an upper and a lower limit, and in the main it was found that the estimates of Nusselt and Peclet groups were not affected by the wide values of the upper and lower limits. However, the sensitivity of the experiments to the thermal conductivity of the glass was not strong, and the standard errors of the thermal conductivity given above were affected by the fairly narrow upper and lower limits that had been estimated from published values, so that the standard errors reported give an optimistic estimate of the accuracy of the method. Most of the experiments that contributed to the average value were taken at Reynolds numbers less than 100. However, the pulse response should be most sensitive to the thermal conductivity of the solid at high Reynolds numbers when the effect of thermal dispersion is reduced, and when the relative magnitude of the external to internal thermal resistance has been reduced by an increase in the heat transfer coefficient. The most accurate values of the intra-particle thermal conductivity should be obtained at high Reynolds numbers.

The performance of all three methods of estimation was comparable in the apparent accuracy of predictions. However, there was a very large difference in computing times for each method. In general the Fourier transform method took almost three times as long as the Laplace transform, but the numerical solution of the partial differential equations was about 100 times as slow as the Laplace transform. Thus the numerical method was demanding in requirement for computer storage and speed although the choice of satisfactory intervals of integration was more straightforward. It is apparent however that if accurate thermal responses have been recorded any one of the three methods of parameter estimation may be used with some confidence, with perhaps the Laplace transform method as the best all round and most economical choice.

Acknowledgement—S.C.D. wishes to acknowledge the award of a study grant administered by the British Council under the auspices of the Colombo Plan.

REFERENCES

1. J. J. Barker, Heat transfer in packed beds, *Ind. Engng Chem.* **57**(4), 43 (1965).
2. D. J. Gunn and J. F. C. de Souza, Heat transfer and axial dispersion in packed beds, *Chem. Engng Sci.* **29**, 1363 (1974).
3. G. A. Turner and L. Otten, Values of thermal (and other) parameters in packed beds, *Ind. Engng Chem. Process. Des. Dev.* **12**, 417 (1973).
4. H. Littman, R. Barile and A. H. Pulsifer, Gas-particle heat transfer coefficients in packed beds at low Reynolds numbers, *Ind. Engng Chem. Fundam.* **7**, 554 (1968).
5. D. J. Gunn, P. V. Narayanan and A. P. Wardle, Heat transfer in fixed beds of particles at low and intermediate Reynolds numbers, *Proc. 6th Int. Heat Transfer Conf.*, Toronto, PI-4, p. 19 (1978).
6. D. J. Gunn, The transient and frequency response of particles and beds of particles, *Chem. Engng Sci.* **25**, 53 (1970).,
7. W. F. Ames, *Numerical Methods for Partial Differential Equations.* Thomas Nelson, London (1969).
8. H. Bashi and D. J. Gunn, The characterization of fixed beds of solids from pulse response, *A.I.Ch.E. Jl* **23**, 40 (1977).
9. D. J. Gunn and C. Pryce, Dispersion in packed beds, *Trans. Instn Chem. Engrs* **47**, 341 (1969).
10. D. J. Gunn and P. V. Narayanan, Axial thermal dispersion and particle to fluid transfer in packed-fluidized beds, *Int. J. Heat Mass Transfer* **24**, 1405 (1981).
11. D. J. Gunn, Transfer of heat or mass to particles in fixed and fluidized beds, *Int. J. Heat Mass Transfer* **21**, 467 (1978).
12. O. L. Davies and P. L. Goldsmith (editors), *Statistical Methods in Research and Production.* Oliver & Boyd, Edinburgh (1972).

ANALYSE DU TRANSFERT THERMIQUE DANS DES LITS FIXES DE PARTICULES A DES NOMBRES DE REYNOLDS BAS OU INTERMEDIAIRES

Résumé—On mesure la réponse dynamique de lits fixes de billes de verre à une impulsion de température, dans un domaine de nombre de Reynolds allant de 1 à 300. La conductivité thermique des particules, le coefficient de transfert entre particule et fluide et le coefficient de dispersion axiale thermique sont obtenus par la transformation de Laplace, la transformation de Fourier et par une méthode numérique, chacune appliquée à une recherche de variance maximale. Les trois méthodes sont décrites et comparées. Un accord est bon dans tout le domaine de nombre de Reynolds bien que la sensibilité à la dispersion axiale soit plus grande aux faibles nombres, tandis que la sensibilité au coefficient de transfert thermique et à la conductivité intraparticulaire soit plus grande aux nombres de Reynolds élevés.

UNTERSUCHUNG DES WÄRMEÜBERGANGS IN FESTBETTSCHÜTTUNGEN BEI KLEINEN UND MITTLEREN REYNOLDS-ZAHLEN

Zusammenfassung—Die Sprungantwort eines Festbettes aus kleinen Glaskugeln wurde für Reynolds-Zahlen im Bereich von 1–300 gemessen. Die Wärmeleitfähigkeit der Partikel, der Wärmeübergangskoeffizient zwischen Fluid und Partikeln und der Koeffizient für die axiale Wärmeausbreitung wurden durch Laplace- sowie Fourier-Transformation und eine numerische Methode ermittelt. Die drei Methoden werden beschrieben und verglichen. Über den gesamten Bereich der Reynolds-Zahlen ergab sich eine gute Übereinstimmung, obgleich die Empfindlichkeit der Experimente für die axiale Wärmeausbreitung bei kleinen Reynolds-Zahlen und diejenige für den Wärmeübergangskoeffizienten sowie für die Wärmeleitung zwischen den Partikeln bei hohen Reynolds-Zahlen am größten war.

АНАЛИЗ ТЕПЛОПЕРЕНОСА В НЕПОДВИЖНЫХ СЛОЯХ ЧАСТИЦ ПРИ МАЛЫХ И ПРОМЕЖУТОЧНЫХ ЗНАЧЕНИЯХ ЧИСЛА РЕЙНОЛЬДСА

Аннотация—Реакция динамической системы на возмущения, вызванные наложением входного импульса на неподвижные слои стеклянных частиц, измерялась в диапазоне значений чисел Рейнольдса для частиц от 1 до 300. Теплопроводность частиц, коэффициент теплопереноса от частиц к жидкости и коэффициент аксиального рассеяния тепла определялись с помощью преобразований Лапласа и Фурье, а также численным методом, причем каждый применялся для отыскания минимальной дисперсии. Дано описание и проведено сравнение трех методов оценок. Найдено хорошее соответствие результатов во всем диапазоне чисел Рейнольдса, несмотря на то, что при низких значениях чисел Рейнольдса осевое рассеяние тепла оказывало большое влияние на измеряемые результаты, в то время как при больших числах Рейнольдса большое влияние оказывали коэффициент теплопереноса жидкости и теплопроводность между частицами.